Research Article

Hypoxic preconditioning reduces NLRP3 inflammasome expression and protects against cerebral ischemia/reperfusion injury

https://doi.org/10.4103/1673-5374.314317

Date of submission: December 2, 2020

Date of decision: January 29, 2021

Date of acceptance: April 2, 2021

Date of web publication: July 8, 2021

Yi-Qiang Pang[1, 2], Jing Yang[3], Chun-Mei Jia[2], Rui Zhang[1], Qi Pang[1, *]

Graphical Abstract *Hypoxic preconditioning prevents the cerebral ischemia/reperfusion (I/R) injury through reducing the NOD-like receptor family pyrin domain containing 3 (NLRP3) inflammasome expression*

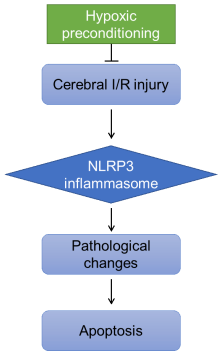

Abstract

Hypoxic preconditioning can protect against cerebral ischemia/reperfusion injury. However, the underlying mechanisms that mediate this effect are not completely clear. In this study, mice were pretreated with continuous, intermittent hypoxic preconditioning; 1 hour later, cerebral ischemia/reperfusion models were generated by middle cerebral artery occlusion and reperfusion. Compared with control mice, mice with cerebral ischemia/reperfusion injury showed increased Bederson neurological function scores, significantly increased cerebral infarction volume, obvious pathological damage to the hippocampus, significantly increased apoptosis; upregulated interleukin-1β, interleukin-6, and interleukin-8 levels in brain tissue; and increased expression levels of NOD-like receptor family pyrin domain containing 3 (NLRP3), NLRP inflammasome-related protein caspase-1, and gasdermin D. However, hypoxic preconditioning significantly inhibited the above phenomena. Taken together, these data suggest that hypoxic preconditioning mitigates cerebral ischemia/reperfusion injury in mice by reducing NLRP3 inflammasome expression. This study was approved by the Medical Ethics Committee of the Fourth Hospital of Baotou, China (approval No. DWLL2019001) in November 2019.

Key Words: apoptosis; caspase-1; cell death; cerebral ischemia/reperfusion injury; gasdermin D; hippocampus; hypoxic preconditioning; NLRP3 inflammasome

Chinese Library Classification No. R454.4; R741.05; R364.5

Introduction

In China, the death rate associated with cerebrovascular diseases was recently reported at 149.49 per 100,000 population (Wang et al., 2020c). The only effective treatment for cerebral ischemic disease is the rapid restoration of the blood flow to the brain. However, reperfusion often aggravates brain injury, resulting in cerebral ischemia/reperfusion (I/R) injury (Kalogeris et al., 2012). Therefore, during the treatment of cerebral ischemia, the prevention and treatment of subsequent reperfusion injury must be performed simultaneously with the rapid recovery of cerebral tissue through perfusion. The pathophysiological process underlying cerebral I/R injury is complex. Currently, intracellular Ca^{2+} overloading, oxygen free radical injury, excitatory amino acid toxicity, chemokines, and white blood cell interactions are considered to be underlying pathogenic factors that contribute to cerebral I/R injury (L et al., 2016; Min et al., 2020).

Hypoxic preconditioning (HPC) refers to the highly tolerant

[1]Department of Neurosurgery, Shandong Provincial Hospital, Cheeloo College of Medicine, Shandong University, Jinan, Shandong Province, China; [2]Department of Neurosurgery, The Fourth Hospital of Baotou, Baotou, Inner Mongolia Autonomous Region, China; [3]Department of Basic Medicine and Forensic Medicine, Baotou Medical College, Baotou, Inner Mongolia Autonomous Region, China

*Correspondence to: Qi Pang, PhD, doctorpangqi@126.com.

https://orcid.org/0000-0001-5368-8417 (Qi Pang)

Funding: *This work was supported by National Natural Science Foundation of China, No. 81771270 (to QP); Inner Mongolia Science Foundation of China, No. 2020MS08063 (to YQP); Health and Family Planning Scientific Research Plan Project of Inner Mongolia Autonomous Region of China, No. 201702138 (to YQP); Baotou Science and Technology Plan Project of China, No. 2018C2007-4-10 (to YQP); Baotou Medical and Health Science and Technology Project of China, No. wsjj2019036 (to JY); and Baotou Medical College Foundation of China, No. BSJJ201904 (to JY).*

How to cite this article: *Pang YQ, Yang J, Jia CM, Zhang R, Pang Q (2022) Hypoxic preconditioning reduces NLRP3 inflammasome expression and protects against cerebral ischemia/reperfusion injury. Neural Regen Res 17(2):395-400.*

treatment of long-term lethal I/R injury through exposure to intermittent, repeated, short-term, non-lethal hypoxic stress. HPC has been reported to ameliorate I/R injury not only in the brain but also in the myocardial tissue (Tang et al., 2009). The potential mechanisms underlying HPC include autophagy induction and apoptosis inhibition (Zhang et al., 2017; Liu et al., 2020).

Inflammation is a biological response through which body tissues prevent the effects mediated by harmful stimuli (Chen et al., 2018; Mo et al., 2020). However, excessive inflammatory reactions can be harmful to neurons (Song et al., 2020; Zhang et al., 2020b). Inflammasomes are multiprotein complexes that are important components of the innate immune system and regulate inflammatory reactions. The NOD-like receptor family pyrin domain containing 3 (NLRP3) inflammasome acts as a cytoplasmic pattern recognition receptor that can recognize various exogenous pathogens and sense endogenous risk signals, linking the innate immune response with the acquired immune response (Heneka et al., 2013; Coll et al., 2015). The NLRP3 inflammasome plays an important role in cerebral I/R injury (Wang et al., 2020a). However, whether the NLRP3 inflammasome is involved in the HPC-mediated protection against cerebral I/R injury remains unknown.

In this study, mice were treated with HPC followed by the generation of a cerebral I/R injury model to clarify the protective effects of HPC and to assess the involvement of the NLRP3 inflammasome in the potential underlying mechanisms.

Materials and Methods

Animals

A total of 45 male, specific-pathogen-free-grade BALB/c mice, aged 2 months and weighing 20–22 g, were purchased from Hunan SLYK Jingda Experimental Animal Co., Ltd., China [licence No. SCXK (Xiang) 2019-0004]. The experimental animal protocol was approved by the Medical Ethics Committee of the Fourth Hospital of Baotou, China (approval No. DWLL2019001; approval date: November 2019). All experiments were designed and reported according to the Animal Research: Reporting of *In Vivo* Experiments (ARRIVE) guidelines.

To avoid the potentially confounding influence of estrogen, this study used only male mice. A total of 45 male mice were used, and three animals died during cerebral I/R injury modeling. All animals were maintained in a specific pathogen-free environment at 23 ± 2°C and relative humidity of 45–65% under a controlled 12-hour light/dark cycle. All mice had free access to food and water. During the first part of this experiment, the mice were randomly divided into three groups (n = 6 per group): HPC + 1 hour of ischemia followed by 12, 24, and 36 hours of reperfusion (HPC + I/R 12-hour, HPC + I/R 24-hour, and HPC + I/R 36-hour groups, respectively). The follow-up experiments were conducted using 12-hour I/R conditions. Mice in the follow-up experiments were randomly divided into the following experimental groups (n = 6 per group): sham operation (control), HPC (HPC + sham), I/R, and HPC + I/R groups.

HPC

HPC was administered, as previously described (Cui et al., 2004). Briefly, the mice were placed in a 125-mL wide-mouth bottle containing fresh air. Immediately after the mice were placed in the bottle, the bottle mouth was closed with a rubber stopper, and the first observation of asthmatic breathing was taken as an index of the end of each hypoxic exposure. The tolerance times of the mice were recorded, and the mice were removed immediately; this procedure was considered one incidence of hypoxic exposure (H1), then transferred to another wide-mouth bottle with the same volume of fresh air. The second hypoxic exposure was recorded as H2, followed by the third (H3) and the fourth (H4) exposures using the same protocol. When the tolerance time of the second, third, and fourth hypoxic exposure reached two, four, and six times the tolerance time of the first hypoxia exposure, the hypoxic exposure was ceased.

Cerebral I/R models

One hour after HPC exposure, middle cerebral artery occlusion was performed under inhalation anesthesia with isoflurane (RWD, Shenzhen, China; 5% induction, 1% maintenance), as previously described (Longa et al., 1989). A midline incision was prepared along the ventral side of the neck under a stereomicroscope (Olympus, Tokyo, Japan). The left common carotid artery, internal carotid artery, and external carotid artery were carefully exposed and separated from the vagus nerve. The distal end of the external carotid artery was ligated, and an arteriotomy was performed at the distal end of the external carotid artery. A nylon wire was inserted from the artery incision until it met with slight resistance. After 60 minutes, the occluding filament was gently removed to allow blood flow and reperfusion for 12, 24, and 36 hours. Mice in the sham control group were subjected to the same operation, but no wire was inserted. Cerebral blood flow was monitored using a Doppler flowmeter (Yongan Jixin, Beijing, China). The effects of HPC on NLRP3 following different I/R conditions were evaluated (reperfusion of 12, 24, and 36 hours). During surgery, the body temperatures of all animals were monitored and maintained between 37.0°C and 37.5°C using a heating pad. The mice in each group were sacrificed at the end of the indicted reperfusion period by decapitation under anesthesia with isoflurane. Brain tissues were cryopreserved, and the expression of NLRP3 was detected by western blot assay, as previously described (Song et al., 2019).

Evaluation of neurological function

According to the standards for evaluating the Bederson neurological function score (Bederson et al., 1986), the neurological function of mice was evaluated after 12 hours of reperfusion (**Additional Table 1**). Higher scores indicated more severe injury in the animals. A score of 0 indicated normal neurological function, whereas scores of 1–4 represented neurological dysfunction.

Triphenyl tetrazolium chloride staining

After 12 hours of reperfusion, the animals were anesthetized. After complete anesthesia, the heart was perfused with 10 mL normal saline; the whole brain tissue was frozen at –20°C for approximately 30 minutes. The cerebellum and olfactory bulb were discarded, and the remaining brain tissue was cut into five continuous slices coronally. The brain slices were placed in a closed container with 2% triphenyl tetrazolium chloride solution and incubated in the dark for 15 minutes at 37°C. During this period, the brain slices were flipped every 5 minutes to ensure even staining. The relative infarct area was calculated based on the following formula: relative infarct area (%) = infarct area/total area of the brain.

Hematoxylin-eosin staining

Neuronal morphology was detected using hematoxylin-eosin staining. After 12 hours of reperfusion, brain tissues were isolated and fixed in 4% paraformaldehyde overnight, followed by dehydration in 70%, 80%, and 90% ethanol solution, a mixture of alcohol and xylene for 15 minutes, xylene I for 15, minutes and xylene II for 15 minutes. The sections were incubated in a mixture of xylene and paraffin for 15 minutes, followed by paraffin I and paraffin II, for 50–60 minutes, each. The tissues were paraffin-embedded and sectioned into 10-μm slices. The paraffin-embedded sections were dewaxed and hydrated. After being rinsed in distilled water, the slices were dyed with hematoxylin solution for 3 minutes, differentiated by hydrochloric acid alcohol differentiation solution for 15

seconds, washed slightly, and returned to eosin solution for 15 seconds. Images were obtained using a light microscope (Olympus), and pathological changes in the hippocampus were analyzed.

Enzyme-linked immunosorbent assay
After 12 hours of reperfusion, the animals were anesthetized, and brain tissues were collected for further use. The levels of cytokine expression in the brain tissue were detected using the indicated assay kits, according to the manufacturer's instructions, as previously described (Yang et al., 2019): interleukin (IL)-8 assay kit (Cat# MM-0123M1, Meilian Bio, Shanghai, China), IL-6 assay kit (Cat# MM-0163M1, Meilian Bio), and IL-1β assay kit (Cat# MM-0040M1, Meilian Bio).

Terminal-deoxynucleotidyl transferase-mediated nick-end labeling staining
After 12 hours of reperfusion, the animals were anesthetized. Brain tissues were collected and fixed in 4% paraformaldehyde at 4°C overnight. The brain tissues were embedded in paraffin, and 3-μm sections were continuously sliced. The paraffin sections were placed in an oven at 65°C for 2 hours, incubated in xylene for 10 minutes, and then incubated in 100% ethanol, 95% ethanol, 80% ethanol, and purified water for 5 minutes each. The slices were transferred into a wet box, 50 μg/mL protein K working solution was added, and the reaction was conducted at 37°C for 30 minutes. The sample was fully washed three times with phosphate-buffered saline (PBS). Residual PBS around the tissue was removed with absorbent paper, and an excessive volume of terminal-deoxynucleotidyl transferase-mediated nick-end labeling detection solution was dripped onto the slice and incubated at 45°C for 2 hours, followed by three washes with PBS. An anti-fluorescence quenching seal was used, and slices were examined under a fluorescence microscope (Olympus). The apoptotic rate was calculated using the formula: apoptotic rate (%) = Number of terminal-deoxynucleotidyl transferase-mediated nick-end labeling-stained cells (green)/number of DAPI-stained cells (blue) × 100.

Immunofluorescence
After 12 hours of reperfusion, the animals were anesthetized. Brain tissues were collected and fixed in 4% paraformaldehyde at 4°C overnight. The tissues were cryoprotected in 30% sucrose for 1 hour at 4°C and sectioned on a freezing microtome (Leica, Munich, Germany) at 20 μm. The slices were heated and boiled in citric acid buffer for 2 minutes and then washed with PBS after natural cooling. The slices were transferred into a wet box, incubated with 5% bovine serum albumin, and sealed at 37°C for 30 minutes. After removing the blocking solution, rabbit anti-NLRP3 antibody (1:100, Cat# bs-10021R, Bioss, Beijing, China) was added as the primary antibody and incubated at 37°C for 3 hours. The fluorescent goat anti-rabbit IgG-Fluor-488 (1:200; Cat# ZB-2301, ZSGB-BIO, Beijing, China) was added and incubated at 37°C for 30 minutes. Nuclei were stained with 4′,6-diamidino-2-phenylindole (Beyotime, Ningbo, China), and images were obtained using fluorescence microscopy. The fluorescence intensity of NLRP3 was calculated using ImageJ software.

Western blot assay
After 12 hours of reperfusion, the animals were anesthetized. Brain tissues were collected, and lysates were obtained, as previously described (Song et al., 2019). After 30 minutes on ice, the tissues were centrifuged at 4°C and 10,000 r/min for 10 minutes. The supernatant was carefully aspirated to obtain the total protein. The protein concentration was determined using a bicinchoninic acid kit (Beyotime, Beijing, China). The proteins underwent denaturation in a boiling water bath, and the samples were separated by sodium dodecyl sulfate-polyacrylamide gel electrophoresis (10% gel) for 1–2 hours, followed by wet transfer to a nitrocellulose membrane for 30–50 minutes. The membranes were blocked by 5% non-fat milk at room temperature for 2 hours and then incubated with the following primary antibodies at 4°C overnight: rabbit anti-NLRP3 antibody (1:100, Cat# bs-10021R, Bioss), rabbit anti-Caspase-1 antibody (1:1000, Cat# AF5418, Affinity, Cincinnati, OH, USA), rabbit anti-gasdermin D (GSDMD) antibody (1:1000, Cat# AF4012, Affinity), and rabbit anti-β-actin (1:100, Cat# bs-0061R, Bioss). The membranes were then incubated with goat anti-rabbit IgG/horseradish peroxidase antibody (1:200, Cat# bs-0295G-HRP, Bioss) at room temperature for 1–2 hours. An enhanced chemiluminescence exposure solution (Thermo Fisher Scientific, Inc., Shanghai, China) was added to the membrane and visualized using a gel imaging system (Bio-Rad, Shanghai, China). The optical density of each band was analyzed by Quantity One Software (Bio-Rad).

Statistical analysis
All data were processed using SPSS 19.0 (IBM Corp., Armonk, NY, USA). Data are expressed as the mean ± standard deviation (SD). Significant differences among groups were analyzed by one-way analysis of variance followed by Tukey's *post hoc* test. A value of $P < 0.05$ was considered significant.

Results

HPC prevents cerebral I/R injury
As shown in **Figure 1A**, four stages of HPC were examined in mice. The time of tolerance limits used for the second, third, and fourth hypoxia exposures were approximately two, four, and six times the tolerance time established during the first hypoxia exposure ($F_{(3, 20)} = 89.68$, $P < 0.05$), indicating that the HPC effect was suitable, and the adaptability of mice to a hypoxic environment was enhanced.

Figure 1B shows the western blot analysis of NLRP3 protein expression in brain tissue after HPC combined with different I/R protocols. As shown in **Figure 1B**, NLRP3 expression levels increased with increased reperfusion time ($F_{(2, 15)} = 3639$, $P < 0.05$), which indicated that the NLRP3 inflammasome was involved in the regulation of HPC.

The Bederson neurological function score of the I/R group was 3.5 ± 0.58, which was significantly higher than those for the sham and HPC groups (scores of 0), indicating that the neurological function of the I/R mice was damaged and that limb activity was abnormal. The Bederson neurological function score of the HPC + I/R group was 2.5 ± 0.58, which was significantly lower than that of the I/R group, indicating that HPC was able to reduce the effects of I/R injury in mice. The results of triphenyl tetrazolium chloride staining (**Figure 2**) showed that the infarct area of the I/R group was remarkably larger than that in the sham group, whereas only a slight infarct area was observed in the HPC + I/R group ($F_{(3, 20)} = 337.8$, $P < 0.05$).

HPC prevents neuronal apoptosis in the hippocampus of cerebral I/R injury model mice
As shown in **Figure 3**, the hematoxylin-eosin staining results showed that the hippocampal morphologies of the control and HPC groups were complete, with regularly arranged cortical cells and a clear structure. After I/R modeling, the hippocampus was obviously damaged, including fuzzy structures, irregular arrangements, and the infiltration of inflammatory cells. Compared with the I/R group, the pathological changes observed in the HPC + I/R group were significantly improved. Terminal-deoxynucleotidyl transferase-mediated nick-end labeling assay showed that the number of apoptotic cells was significantly increased in the I/R group than in the control group, whereas the apoptosis of the hippocampal cells was significantly decreased in the HPC + I/R group compared with that in the I/R group ($F_{(3, 20)} = 55.21$, $P < 0.05$; **Figure 4**).

HPC prevents cytokine release in the brains of cerebral I/R injury model mice

As shown in **Figure 5**, the cytokine contents, including IL-1β, IL-6, and IL-8, were measured in the brain tissues of mice using enzyme-linked immunosorbent assays. Compared with that of the control group, the IL-1β content of the I/R group significantly increased. HPC treatment significantly reduced the levels of IL-1β ($F_{(3, 20)}$ = 117, P < 0.05), IL-6 ($F_{(3, 20)}$ = 77.32, P < 0.05), and IL-8 ($F_{(3, 20)}$ = 90.04, P < 0.05) compared with those in the I/R group.

HPC prevents the formation of the NLRP3 inflammasome in cerebral I/R injury model mice

As shown in **Figure 6**, the expression levels of caspase-1, GSDMD, and NLRP3 were detected by western blot assay to represent the expression of the NLRP3 inflammasome. The expression levels of caspase-1 ($F_{(3, 20)}$ = 1113, P < 0.05), GSDMD ($F_{(3, 20)}$ = 403.7, P < 0.05), and NLRP3 ($F_{(3, 20)}$ = 756.2, P < 0.05) were significantly increased in the I/R group compared with those in the control group, whereas those in the HPC + I/R group were significantly reduced compared with those in the I/R group. The immunopositivity of NLRP3, as determined by immunofluorescence analysis, was similar to the results observed in the western blot assay. The immunopositivity of NLRP3 in the I/R group was significantly increased compared with that in the control group, whereas that in the HPC + I/R group was significantly reduced compared with that in the I/R group ($F_{(3, 20)}$ = 982.2, P < 0.05; **Figure 7**).

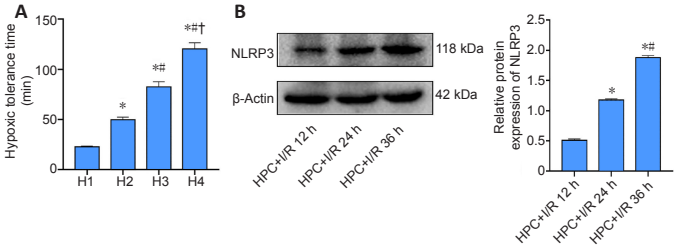

Figure 1 | **Validation of hypoxic preconditioning and NLRP3 expression in I/R model mice.**
(A) Comparison of the tolerance times measured for the four stages of hypoxic preconditioning. (B) The expression of NLRP3 in the brains of I/R model mice. The protein expression was normalized against that of β-actin. Data are expressed as the mean ± SD (n = 6). *P < 0.05, *vs*. H1 or HPC + I/R 12-hour group; #P < 0.05, *vs*. H2 or HPC + I/R 24-hour group; †P < 0.05, *vs*. H3 (one-way analysis of variance followed by Tukey's *post hoc* test). 12 h: 12-hour reperfusion; 24 h: 24-hour reperfusion; 36 h: 36-hour reperfusion. H1–4: The first, second, third, and fourth hypoxic exposure events; HPC: hypoxic preconditioning; I/R: ischemia/reperfusion; NLRP3: NOD-like receptor family pyrin domain containing 3.

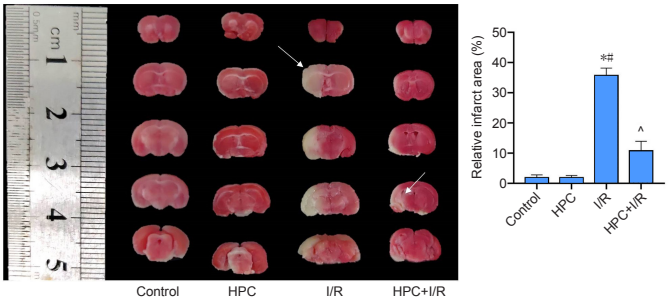

Figure 2 | **Effect of HPC on the infarct area in mice subjected to cerebral I/R injury.**
Triphenyl tetrazolium chloride staining showed infarct areas as gray-white (arrows) and non-infarct areas as dark red. The infarct area in the I/R group was remarkably increased compared with that in the control group, whereas only a slight infarct area was observed in the I/R model after hypoxic preconditioning. Data are expressed as the mean ± SD (n = 6). *P < 0.05, *vs*. control group; #P < 0.05, *vs*. HPC group; ^P < 0.05, *vs*. I/R group (one-way analysis of variance followed by Tukey's *post hoc* test). HPC: Hypoxic preconditioning; I/R: ischemia/reperfusion.

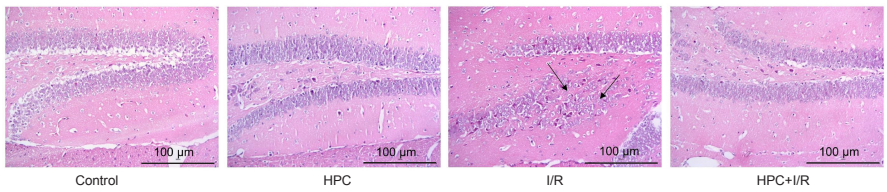

Figure 3 | **Effect of HPC on the hippocampal morphology in mice subjected to cerebral I/R injury, as detected by hematoxylin-eosin staining.**
The hippocampal morphology of the control and HPC groups was complete. The cortical cells were arranged regularly, and the structure was clear. After I/R modeling, the hippocampus was obviously damaged, presenting a fuzzy structure, irregular arrangement, and the infiltration of inflammatory cells (arrows). Arrows indicated the infiltration of inflammatory cells. Scale bars: 100 μm. Original magnification, 400×. HPC: Hypoxic preconditioning; I/R: ischemia/reperfusion.

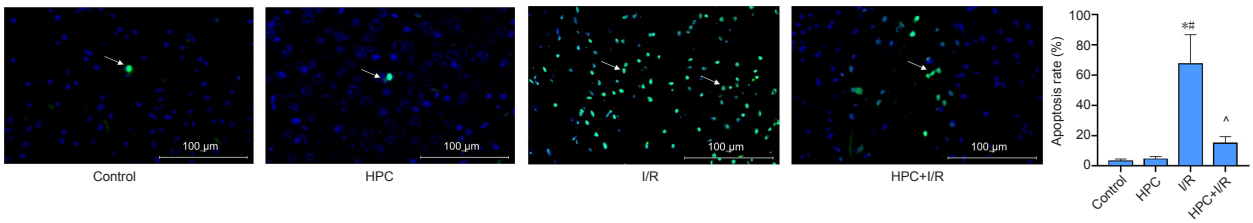

Figure 4 | **Effect of HPC on neuronal apoptosis in the brains of cerebral I/R injury model mice.**
Terminal-deoxynucleotidyl transferase-mediated nick-end labeling assay showed that the number of apoptotic cells (arrows) in the I/R group was significantly higher than that in the control group, whereas the number of apoptotic hippocampal cells in the HPC + I/R group was significantly decreased compared with that in the I/R group. Scale bars: 100 μm. Data are expressed as the mean ± SD (n = 6). *P < 0.05, *vs*. control group; #P < 0.05, *vs*. HPC group; ^P < 0.05, *vs*. I/R group (one-way analysis of variance followed by Tukey's *post hoc* test). HPC: Hypoxic preconditioning; I/R: ischemia/reperfusion.

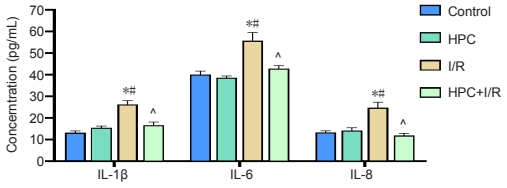

Figure 5 | **Effect of HPC on cytokine release in the brains of cerebral I/R injury model mice.**
The contents of cytokines, including IL-1β, IL-6, and IL-8, were detected in the brain tissues of mice by enzyme-linked immunosorbent assay. Compared with those in the control group, the contents of IL-1β, IL-6, and IL-8 in the I/R model group were significantly increased, whereas these were significantly reduced by HPC. Data are expressed as the mean ± SD (n = 6). *P < 0.05, *vs*. control group; #P < 0.05, *vs*. HPC group; ^P < 0.05, *vs*. I/R group (one-way analysis of variance followed by Tukey's *post hoc* test). HPC: Hypoxic preconditioning; I/R: ischemia/reperfusion; IL: interleukin.

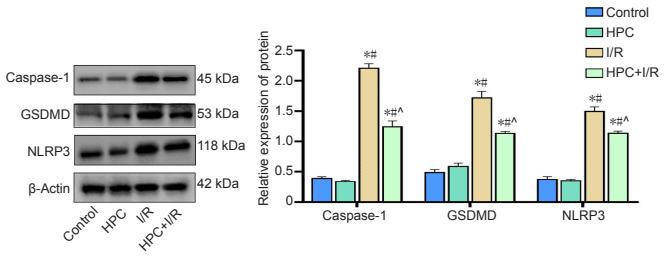

Figure 6 | **Effect of HPC on the expression of caspase-1, GSDMD, and NLRP3 in the brains of cerebral I/R injury model mice.**
The expression levels of caspase-1, GSDMD, and NLRP3 were significantly increased in the I/R group compared with those in the control group, whereas those in the HPC + I/R group were significantly decreased compared with those in the I/R group. Data are expressed as the mean ± SD (n = 6). *P < 0.05, *vs*. control group; #P < 0.05, *vs*. HPC group; ^P < 0.05, *vs*. I/R group (one-way analysis of variance followed by Tukey's *post hoc* test). GSDMD: Gasdermin D; HPC: hypoxic preconditioning; I/R: ischemia/reperfusion; NLRP3: NOD-like receptor family pyrin domain containing 3.

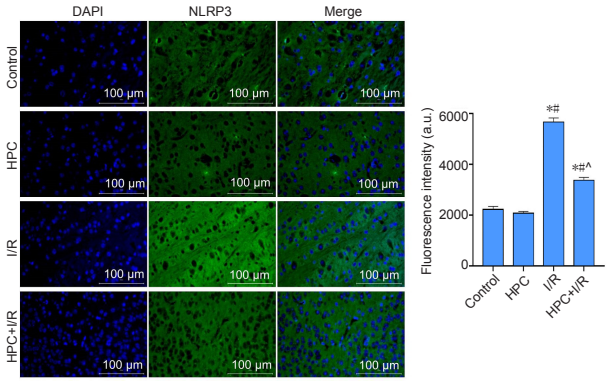

Figure 7 | **Effect of HPC on the fluorescence intensity of NLRP3 in the brains of cerebral I/R injury model mice, as detected by immunofluorescence.**
The fluorescence intensity of NLRP3 in the I/R group was significantly increased compared with that in the control group, whereas that in the HPC + I/R group was significantly lower than that in the I/R group. Scale bars: 100 μm. Data are expressed as the mean ± SD (n = 6). *P < 0.05, *vs.* control group; #P < 0.05, *vs.* HPC group; ^P < 0.05, *vs.* I/R group (one-way analysis of variance followed by Tukey's *post hoc* test). DAPI: 4′,6-Diamidino-2-phenylindole; GSDMD: gasdermin D; HPC: hypoxic preconditioning; I/R: ischemia/reperfusion; NLRP3: NOD-like receptor family pyrin domain containing 3.

Discussion

HPC can trigger the expression of a variety of protective factors, such as hypoxia-inducible factor-1α, erythropoietin, and vascular endothelial growth factor (Vellimana et al., 2020; Zhang et al., 2020a). These cytokines can improve the hypoxia tolerance of neurons through different mechanisms (Huang et al., 2014; Zhu et al., 2014). As an endogenous protective mechanism, HPC protects against neuronal injury (Fan et al., 2020). In this study, we first determined the successful establishment of HPC. Second, we found that NLRP3 expression increased with increased reperfusion time. Finally, we evaluated the functional effects of HPC for the protection against cerebral I/R injury. Our results indicated that HPC could reduce cerebral I/R injury and NLRP3 inflammasome expression levels in mice.

Excessive inflammatory reactions are detrimental to synaptic growth, which can result in the development of brain diseases (Amor et al., 2010; Wang et al., 2020b), such as Alzheimer's disease and depression. Cerebral I/R injury can cause excessive inflammatory reactions in brain tissue, which is an important mechanism of brain reperfusion injury (Pei et al., 2015). A large number of inflammatory cells (leukocytes, microglia, and astrocytes) and inflammatory mediators (cytokines, chemokines, and adhesion molecules) participate in the inflammatory reaction (Sochocka et al., 2017). In this study, NLRP3 expression was upregulated following I/R injury, especially among mice that underwent 36 hours of reperfusion.

Pyroptosis is a newly discovered mechanism of programmed cell death, accompanied by inflammatory reactions. Pyroptosis shares morphological characteristics with both necrosis and apoptosis (Cookson and Brennan, 2001). However, unlike apoptosis, during pyroptosis, many 1–2 nm pores form on the cell membrane, resulting in the loss of cell membrane integrity, disrupting the ability to regulate the entry and exit of substances. Eventually, the cell membrane dissolves completely, releasing the cellular contents and inducing an inflammatory reaction. Simultaneously, cells release IL-1β, resulting in the attraction of additional inflammatory cells, which expand the inflammatory response (Fann et al., 2018). In the present study, the IL-1β, IL-6, and IL-8 contents induced by I/R were significantly reduced by HPC. Moreover, neuronal apoptosis was also reduced by HPC. These results, together, imply that pyroptosis during cerebral I/R injury might be prevented by HPC. However, this finding must be verified by additional experiments.

GSDMD is known as a killer protein that mediates cell death and can independently mediate the release of inflammatory mediators, such as IL-1β, in addition to initiating cell membrane rupture and disintegration (He et al., 2015). Pro-caspase-1 is indirectly associated with the pattern recognition receptor NLRP3 via the adaptor protein adaptor-associated speck-like protein, which forms a macromolecular complex known as the caspase-1-dependent inflammasome. After activation by inflammatory mediators, such as IL-1β, inflammatory corpuscles further activate GSDMD and induce programmed cell necrosis (Saito et al., 2015). In studies in which the GSDMD gene was knocked out by gene-editing technology, macrophages were unable to initiate pyroptosis following induction by LPS and known inflammatory body agonists, indicating that GSDMD is a key pyroptosis gene (Kayagaki et al., 2015). The protein expression levels of caspase-1, GSDMD, and NLRP3 were detected by western blot assay, which demonstrated that HPC treatment reduced the expression levels of these three proteins. On the basis of the results from this study, we predict that HPC may inhibit the expression of inflammatory factors or other proteins that are active in the NLRP3 inflammasome pathway.

In our experiments, we identified serious injury to the brain tissue 12 hours after reperfusion, although a previous study suggested that 36 hours of reperfusion were necessary to induce severe injury (Huang et al., 2018). However, the death rate after 36 hours of reperfusion in our experiment was high. To reduce the death rate, we selected the 12-hour reperfusion protocol. In the present study, we identified an obvious protective effect of HPC against I/R injury. This study also had some limitations. This study used an HPC pre-treatment that is not feasible in the event of stroke-mediated I/R injury. In our future studies, we will plan to examine whether HPC can mediate the degree of I/R injury after infarction has occurred. Additionally, we only examined male mice in our study. Whether HPC exhibits similar functions in female mice remains unknown because estrogenic effects in female mice might influence the functions of HPC.

In conclusion, HPC prevented cerebral I/R injury in mice, likely through the reduction of NLRP3 inflammasome expression. This study suggested that HPC could serve as a potential measure to prevent cerebral I/R injury.

Author contributions: *Study design and manuscript drafting: QP; experimental implementation and data analysis: YQP, JY, CMJ, RZ. All authors read and approved the manuscript and agree to be accountable*

for all aspects of the research in ensuring that the accuracy or integrity of any part of the work are appropriately investigated and resolved.

Conflicts of interest: *The authors declare that they have no competing interests.*

Financial support: *This work was supported by National Natural Science Foundation of China, No. 81771270 (to QP); Inner Mongolia Science Foundation of China, No. 2020MS08063 (to YQP); Health and Family Planning Scientific Research Plan Project of Inner Mongolia Autonomous Region of China, No. 201702138 (to YQP); Baotou Science and Technology Plan Project of China, No. 2018C2007-4-10 (to YQP); Baotou Medical and Health Science and Technology Project of China, No. wsjj2019036 (to JY); and Baotou Medical College Foundation of China, No. BSJJ201904 (to JY). The funding sources had no role in study conception and design, data analysis or interpretation, paper writing or deciding to submit this paper for publication.*

Institutional review board statement: *The study was approved by the Medical Ethics Committee of the Fourth Hospital of Baotou, China (approval No. DWLL2019001) in November 2019.*

Data sharing statement: *Datasets analyzed during the current study are available from the corresponding author on reasonable request.*

Plagiarism check: *Checked twice by iThenticate.*

Peer review: *Externally peer reviewed.*

Additional file:

Additional Table 1: *Longa's neurological function score.*

References

Amor S, Puentes F, Baker D, van der Valk P (2010) Inflammation in neurodegenerative diseases. Immunology 129:154-169.

Bederson JB, Pitts LH, Tsuji M, Nishimura MC, Davis RL, Bartkowski H (1986) Rat middle cerebral artery occlusion: evaluation of the model and development of a neurologic examination. Stroke 17:472-476.

Chen L, Deng H, Cui H, Fang J, Zuo Z, Deng J, Li Y, Wang X, Zhao L (2018) Inflammatory responses and inflammation-associated diseases in organs. Oncotarget 9:7204-7218.

Coll RC, Robertson AA, Chae JJ, Higgins SC, Muñoz-Planillo R, Inserra MC, Vetter I, Dungan LS, Monks BG, Stutz A, Croker DE, Butler MS, Haneklaus M, Sutton CE, Núñez G, Latz E, Kastner DL, Mills KH, Masters SL, Schroder K, et al. (2015) A small-molecule inhibitor of the NLRP3 inflammasome for the treatment of inflammatory diseases. Nat Med 21:248-255.

Cookson BT, Brennan MA (2001) Pro-inflammatory programmed cell death. Trends Microbiol 9:113-114.

Cui XY, Li JF, Han S, Zu PY (2004) Hypoxic preconditioning increases cPKCgamma membrane translocation in murine brain. Sheng Li Xue Bao 56:461-465.

Fan X, Wang H, Zhang L, Tang J, Qu Y, Mu D (2020) Neuroprotection of hypoxic/ischemic preconditioning in neonatal brain with hypoxic-ischemic injury. Rev Neurosci doi: 10.1515/revneuro-2020-0024.

Fann DY, Lim YA, Cheng YL, Lok KZ, Chunduri P, Baik SH, Drummond GR, Dheen ST, Sobey CG, Jo DG, Chen CL, Arumugam TV (2018) Evidence that NF-κB and MAPK signaling promotes NLRP inflammasome activation in neurons following ischemic stroke. Mol Neurobiol 55:1082-1096.

He WT, Wan H, Hu L, Chen P, Wang X, Huang Z, Yang ZH, Zhong CQ, Han J (2015) Gasdermin D is an executor of pyroptosis and required for interleukin-1β secretion. Cell Res 25:1285-1298.

Heneka MT, Kummer MP, Stutz A, Delekate A, Schwartz S, Vieira-Saecker A, Griep A, Axt D, Remus A, Tzeng TC, Gelpi E, Halle A, Korte M, Latz E, Golenbock DT (2013) NLRP3 is activated in Alzheimer's disease and contributes to pathology in APP/PS1 mice. Nature 493:674-678.

Huang JL, Liu WW, Sun XJ (2018) Hydrogen inhalation improves mouse neurological outcomes after cerebral ischemia/reperfusion independent of anti-necroptosis. Med Gas Res 8:1-5.

Huang T, Huang W, Zhang Z, Yu L, Xie C, Zhu D, Peng Z, Chen J (2014) Hypoxia-inducible factor-1α upregulation in microglia following hypoxia protects against ischemia-induced cerebral infarction. Neuroreport 25:1122-1128.

Kalogeris T, Baines CP, Krenz M, Korthuis RJ (2012) Cell biology of ischemia/reperfusion injury. Int Rev Cell Mol Biol 298:229-317.

Kayagaki N, Stowe IB, Lee BL, O'Rourke K, Anderson K, Warming S, Cuellar T, Haley B, Roose-Girma M, Phung QT, Liu PS, Lill JR, Li H, Wu J, Kummerfeld S, Zhang J, Lee WP, Snipas SJ, Salvesen GS, Morris LX, et al. (2015) Caspase-11 cleaves gasdermin D for non-canonical inflammasome signalling. Nature 526:666-671.

L L, X W, Z Y (2016) Ischemia-reperfusion injury in the brain: mechanisms and potential therapeutic strategies. Biochem Pharmacol (Los Angel) 5:213.

Liu N, Zhang XL, Jiang SY, Shi JH, Cui JH, Liu XL, Han LH, Gong KR, Yan SC, Xie W, Zhang CY, Shao G (2020) Neuroprotective mechanisms of DNA methyltransferase in a mouse hippocampal neuronal cell line after hypoxic preconditioning. Neural Regen Res 15:2362-2368.

Longa EZ, Weinstein PR, Carlson S, Cummins R (1989) Reversible middle cerebral artery occlusion without craniectomy in rats. Stroke 20:84-91.

Min DY, Li HY, Guan L, Chang J, Zhang HN, Cui XY, Wang P, Cao YG (2020) Protective mechanism of Naoxinqing Capsule in rat models of cerebral ischemia/reperfusion injury. Zhongguo Zuzhi Gongcheng Yanjiu 24:215-222.

Mo Y, Sun YY, Liu KY (2020) Autophagy and inflammation in ischemic stroke. Neural Regen Res 15:1388-1396.

Pei J, You X, Fu Q (2015) Inflammation in the pathogenesis of ischemic stroke. Front Biosci (Landmark Ed) 20:772-783.

Saito M, Iannaccone A, Kaye G, Negishi K, Kosmala W, Marwick TH (2015) Effect of right ventricular pacing on right ventricular mechanics and tricuspid regurgitation in patients with high-grade atrioventricular block and sinus rhythm (from the protection of left ventricular function during right ventricular pacing study). Am J Cardiol 116:1875-1882.

Sochocka M, Diniz BS, Leszek J (2017) Inflammatory response in the CNS: friend or foe? Mol Neurobiol 54:8071-8089.

Song Z, Shen F, Zhang Z, Wu S, Zhu G (2020) Calpain inhibition ameliorates depression-like behaviors by reducing inflammation and promoting synaptic protein expression in the hippocampus. Neuropharmacology 174:108175.

Song ZJ, Yang SJ, Han L, Wang B, Zhu G (2019) Postnatal calpeptin treatment causes hippocampal neurodevelopmental defects in neonatal rats. Neural Regen Res 14:834-840.

Tang YL, Zhu W, Cheng M, Chen L, Zhang J, Sun T, Kishore R, Phillips MI, Losordo DW, Qin G (2009) Hypoxic preconditioning enhances the benefit of cardiac progenitor cell therapy for treatment of myocardial infarction by inducing CXCR4 expression. Circ Res 104:1209-1216.

Vellimana AK, Aum DJ, Diwan D, Clarke JV, Nelson JW, Lawrence M, Han BH, Gidday JM, Zipfel GJ (2020) SIRT1 mediates hypoxic preconditioning induced attenuation of neurovascular dysfunction following subarachnoid hemorrhage. Exp Neurol 334:113484.

Wang J, Guo M, Ma R, Wu M, Zhang Y (2020a) Tetrandrine alleviates cerebral ischemia/reperfusion injury by suppressing NLRP3 inflammasome activation via Sirt-1. PeerJ 8:e9042.

Wang X, Xu W, Chen H, Li W, Li W, Zhu G (2020b) Astragaloside IV prevents Aβ(1-42) oligomers-induced memory impairment and hippocampal cell apoptosis by promoting PPARγ/BDNF signaling pathway. Brain Res 1747:147041.

Wang YJ, Li ZX, Gu HQ, Zhai Y, Jiang Y, Zhao XQ, Wang YL, Yang X, Wang CJ, Meng X, Li H, Liu LP, Jing J, Wu J, Xu AD, Dong Q, Wang D, Zhao JZ (2020c) China Stroke Statistics 2019: A Report From the National Center for Healthcare Quality Management in Neurological Diseases, China National Clinical Research Center for Neurological Diseases, the Chinese Stroke Association, National Center for Chronic and Non-communicable Disease Control and Prevention, Chinese Center for Disease Control and Prevention and Institute for Global Neuroscience and Stroke Collaborations. Stroke Vasc Neurol 5:211-239.

Yang SJ, Song ZJ, Wang XC, Zhang ZR, Wu SB, Zhu GQ (2019) Curculigoside facilitates fear extinction and prevents depression-like behaviors in a mouse learned helplessness model through increasing hippocampal BDNF. Acta Pharmacol Sin 40:1269-1278.

Zhang J, Zhang J, Li XJ, Xiao J, Ye F (2020a) Hypoxic preconditioning ameliorates amyloid-β pathology and longterm cognitive decline in AβPP/PS1 transgenic mice. Curr Alzheimer Res 17:626-634.

Zhang Z, Song Z, Shen F, Xie P, Wang J, Zhu AS, Zhu G (2020b) Ginsenoside Rg1 prevents PTSD-like behaviors in mice through promoting synaptic proteins, reducing Kir4.1 and TNF-α in the hippocampus. Mol Neurobiol doi: 10.1007/s12035-020-02213-9.

Zhang Z, Yang C, Shen M, Yang M, Jin Z, Ding L, Jiang W, Yang J, Chen H, Cao F, Hu T (2017) Autophagy mediates the beneficial effect of hypoxic preconditioning on bone marrow mesenchymal stem cells for the therapy of myocardial infarction. Stem Cell Res Ther 8:89.

Zhu T, Zhan L, Liang D, Hu J, Lu Z, Zhu X, Sun W, Liu L, Xu E (2014) Hypoxia-inducible factor 1α mediates neuroprotection of hypoxic postconditioning against global cerebral ischemia. J Neuropathol Exp Neurol 73:975-986.

C-Editor: Zhao M; S-Editors: Yu J, Li CH; L-Editors: Giles L, Hindle A, Qiu Y, Song LP; T-Editor: Jia Y

Additional Table 1 Longa's neurological function score

Score	Degree of neurological deficit	Physical activity
0	There was no sign of nerve injury	Physical activity was normal
1	Mild focal injury	The right forelimb cannot fully extend
2	Moderate focal injury	Right rotation when walking
3	Severe focal injury	Tilt to the right when moving autonomously
4	Severe injury	No autonomic activity, accompanied by disturbance of consciousness